Active Retrodirective Arrays

for SPS Beam Pointing

Ralph Chernoff

Jet Propulsion Laboratory

I. INTRODUCTION

The basic requirement of the SPS beam pointing system is that it deliver a certain amount of S-band (λ = 12.5 cm) power to a 9.6 km diameter receiving antenna ("rectenna") on the ground. The power is transmitted from a 1.0 km diameter antenna array on the SPS, which is, for a rectenna at about ±40 deg. latitude, some 37.5×10^6 km distant. Figure 1 shows the "pointing loss", i.e. the relative loss of intercepted power, as a function of pointing error. With perfect pointing the rectenna intercepts 93.5% of the SPS beam, but Figure 1 shows that this falls to 92.6% (1.0% pointing loss) when the pointing error (displacement of peak of beam from rectenna center) is 0.66 km, and 91.6% (2.0% loss) when it is 0.90 km; i.e., pointing loss increases roughly as the square of the pointing error for small errors.[1] 0.66 km is equivalent to $0.66/37.5 \times 10^3$ = 17.6 microradians angular error. At the present time ARA's appear to be the best bet to realize this very stringent beam pointing requirement.

An active retrodirective array (ARA) transmits a beam towards the apparent source of an illuminating signal called the pilot (Figure 3). "Active" implies that the array produces, not merely reflects, RF power. Retro-directivity is achieved by retransmitting from each element of the array a signal whose phase is the "conjugate" of that received by the element. Assuming that the phase of the pilot signal received by the kth element of the array at time t is

$$\phi_k(t) = \omega (t - r_k/c),\tag{1}$$

where r_k is the distance from the κth element to the source of the pilot signal, we define the conjugate of ϕ_k to be

$$\phi_k(t)^* = \omega'(t + r_k/c) + \phi_0\tag{2}$$

where ϕ_0 is an arbitrary phase offset which must, however, be constant over

---

[1] Figure 1 is calculated from two computer programs recently developed at JPL. The first computes the the exact far field power density from a series expansion of the radiation integral for a circular aperture with Gaussian illumination, and the second numerically integrates that power density over the rectenna for various values of the pointing error. The far field program assumes an exact, continuous, Gaussian illumination without phase or amplitude errors. It should not be confused with the program previously developed by W.F. Williams of JPL for the express purpose of simulating the effects of such errors, and which (for that very reason) consumes far more computer time than the present program.

the entire array. In order to do this, each element of the array must be equipped with a phase conjugation circuit (PCC). The phase of the signal received from the κth element by a receiver located at the pilot source ($r = o$) at time t is

$$\phi_k(t,o) = \omega'(t + r_k/c - r_k/c) + \phi_0 = \omega' t + \phi_0. \qquad (3)$$

Thus the contributions to the field at $r = o$ from the various elements of the array are all in phase at that point, which means that the beam points toward the pilot source. Note that this definition does not require that the transmitted frequency, ω', be the same as the pilot frequency. We will, in fact, assume that $\omega' \neq \omega$, as it normally must be in order to provide input-output isolation, but retrodirectivity will still result if the propagation medium is reciprocal and non-dispersive. Note also that the elements of the ARA need be neither equally spaced nor coplanar. The array pattern will, of course, suffer if the array geometry is too irregular, but it will still be retrodirective. Note finally, that the pilot signal wavefront need not be spherical; the ARA will still be retrodirective even if the pilot wavefront is distorted by an inhomogeneous medium provided that the medium is slowly varying (changes negligibly within a round trip light time). In sum, the only necessary conditions for the proper operation of an ARA are that the propagation medium by reciprocal, non-dispersive and slowly varying. The ARA's relative insensitivity to dimensional and propagation medium perturbations makes it highly suitable to the SPS (as well as to a number of other space applications).

An ARA is, to a high degree, inherently failsafe in that failure of the pilot signal results in the immediate collapse of the downlink beam due to the distruction of the phase coherence of the elements of the array. The residual ground level intensity due to the n incoherent signals radiated by an ARA in the absence of a pilot is of order $p/2n$ (depending somewhat on the illumination taper) where n is the number of ARA elements and p is the peak intensity of the beam during normal ARA operation, i.e. in the <u>presence</u> of a pilot signal. For the SPS reference system, $p = 23$ mW/cm^2 and $n = 7200$, so $p/2n$ is about 0.002 mW/cm^3, which is well below levels presently considered hazardous.

II. ARA DESIGN PROBLEMS AND SOLUTIONS

A. Phase Reference Distribution

From (1) and (2) we see that phase conjugation amounts to advancing the phase of an input signal by an amount equal to its delay. The phase conjugation circuit (PCC) must, therefore, be provided with a phase reference against which to measure that delay. If we locate each PCC at its associated ARA element as in Figure 1, then it is clear that we must transmit the phase reference to each PCC from some central source via transmission lines of equal phase delay modulo 2π. But it may be difficult to do this if the transmission lines are very long. For example, consider the 1.0 km diameter SPS ARA described above operating at S-band ($\lambda = 12.5$ cm). If the master phase reference is located at the center of the disk, the transmission lines to elements at the periphery will be 500 m long. If we wish to keep the phase

delay in this line constant to within $\pi/10$ radians, its length must not vary by more than $\pm\lambda/20$ cm, or a relative change no greater than $\pm 1.2 \times 10^{-5}$.

Fortunately, we can avoid the whole problem by locating all PCC's at the reference source rather than at their respective elements. This method of providing the phase reference, called "central phasing", is illustrated in Figure 3, which, for the sake of clarity, shows only two elements of the ARA. The phase reference for this ARA is the pilot signal received by the 0-th, or reference, element. The pilot signal received by the κth element is transmitted to its associated PCC located at the reference element via the transmission line and diplexer, 2PLX. The PCC conjugates the <u>entire</u> phase delay, i.e. the sum of the space delay, $\omega r_k/c$, and the transmission line delay, $\omega \ell_{ko}/c_L$, where c_L is the phase velocity of the line, and transmits that conjugate signal back down the <u>same</u> transmission line to the κth element, which retransmits it. Its phase at that point is $\omega'(t + r_k/c) + \phi_0$ which is exactly what it would be were the PCC located at the κth element rather than at the reference element. Thus the length of the transmission line is immaterial provided only that: 1) the line is dispersionless, and 2) its length is constant with time. Clearly, central phasing is just a simple extension of the phase conjugation principle.

Locating alal the PCC's in one small volume very near the reference element may be difficult if the array contains thousands of elements. A modification of the central phasing idea using a tree topology in which the phase reference is regenerated at each node will be required in such large arrays. This is illustrated in Figure 4. Each branch of the tree consists of a PCC, located near the node, and an element of the ARA at the end of a transmission line. A phase reference supplies all the PCC's connected to a node. At the initial node, this is the reference element of the array. At subsequent nodes, it is a phase reference regenerator (PRR). The PRR combines samples of the pilot and conjugate signals at an element to reproduce the original reference. Specific ways of doing this will be described in the discussion of PCC's in Subsection B below.

The dashed boxes in Figure 4 contain all the circuit elements located at a node. Since the signal paths within these node assemblies are unilateral, their phase delays must be carefully balanced in order to avoid phase error buildup at successive nodes. In order to assure the stability of the phase delay balance, these assemblies must be uniform and compact. Critical applications may require temperature stabilization of some active elements.

The number of nodes in a tree is relatively small even for an ARA of several thousand elements. For example, if we have six branches at each node, then a tree of only five nodes suffices for an array of 9331 elements. PRR's are required only at the first through fourth order nodes of this tree. A PRR at a fourth order node is the last in a chain of four PRR's connecting the PCC's at that fourth order node to the reference element of the ARA. The error in the value of the phase reference produced by this last PRR is the sum of the errors arising in all the PRR's in the chain. If these errors arise from independent and identical random processes in each PRR, then the probable error of the output of the last PRR is $\sqrt{4}$ $(PE)^2 = 2$ (PE) is the probable error of each PRR. Thus the error buildup due to repeated regeneration of the phase reference is moderate even for large arrays.

B. Phase Conjugation Circuits

A very simple phase conjugation circuit (PCC) is shown in Figure 5. Since its input and output frequencies are the same ($\omega'=\omega$), this circuit is impractical because of isolation problems. Shifting the output frequency may solve the isolation problem, but we may, depending on how the shifting is done, find that the transmitted beam is no longer retrodirected. For example, the output frequency of this PCC can be shifted simply by slightly offsetting the frequency of the phase reference by $\Delta\omega$. The result is a sort of approximate phase conjugation which, in a planar ARA, causes a pointing error (called "squint") given by

$$\Delta\theta = -\frac{\Delta\omega}{\omega}\tan\theta, \tag{4}$$

where θ is the scan angle (angle between direction of arrival of the pilot signal and the normal to the array). $\Delta\omega$ has a practical lower bound due to the imperfect isolation of real diplexer filters. Therefore, $\Delta\theta$ may be too large for applications requiring both very precise pointing and a wide scan range.

In order to avoid these difficulties we would like to have <u>exact</u>, frequency shifting PCC's, i.e. PCC's that satisfy our definition, Eq. (2), of phase conjugation where $\omega' \neq \omega$. One such exact PCC is shown in Figure 6. This one uses a phase locked loop which both conjugates the phase and translates the frequency of the input signal. Mixer M2 is an upcoverter while M1 is a downconverter. The conjugate relation,

$$\phi_1^* = R\ (2\ \phi_0 - \phi_1) = R\ \omega\ \left(t + \left(\frac{1}{c}\right)(r_1 - 2\ r_0)\right), \tag{5}$$

where $R = 1/(1 \pm 2/n)$, follows immediately from the phase lock condition. The circuit is practical for $n \geq 4$. The $\pm$ sign in the expression for R reflects the fact that two stable operating states are theoretically possible. Which state actually occurs depends upon the locking range of the VCO. Also, an n-fold phase ambiguity may occur due to the practical difficulty of synchronizing the "divide by n" devices in the various PCC's, but it can be easily shown that this ambiguity is removed (modulo 2π) if the PCC output frequency is multiplied by a multiple of n-2. Since the PCC would normally be designed to operate at frequencies much lower than the 2.45 GHz SPS downlink frequency, the additional requirement that its output frequency be 2450/m(n-2), where m and n-2 are arbitrary positive integers, is not unduly restrictive.

The phase reference regenerator (PRR) for the circuit of Figure 6 may take various forms. One of these is illustrated by the circuit shown in Figure 7 which recovers the phase reference ϕ_0 by the proper combination of the conjugate, $\phi_1^* = R\ (2\ \phi_0 - \phi_1)$, and the pilot signal, ϕ_1. Note that three mixers are required here, not just two; we cannot add two signals of the same frequency in a single mixer because the upper sideband would then have the same frequency as the second harmonic of the strong signal. We must add the pilot signal to the output of M1 in two stages, M2 and M3, in order to remove this "degeneracy".

PCC's and PRR's are, as noted above, usually IF circuits, while the pilot is a microwave signal. We must somehow accurately transfer the phase information in the pilot signal to the IF input signal to the PCC. A receiver which does this is called a coherent receiver. The best known coherent receiver is the phase-locked receiver shown in Figure 8a. The average, or slowly varying, part of the pilot signal phase is divided by n + 1, the ratio of the microwave to IF frequency. A simpler, and much cheaper, kind of coherent receiver is shown in Figure 8b. The pilot signal for this receiver must consist of two carrier signals or "tones" transmitted from the same pilot antenna. These tones can be the upper and lower sidebands produced by balanced modulation. The IF output of the "two-tone receiver" in Figure 8b is simply a doubled version of the modulation, which contains the phase information in each of the pilot tones divided, again, by the pilot/IF frequency ratio. In Figure 8b, we assume that the LO frequency, f_L, lies between those of the two pilot tones, f_1 and f_2, so that mixer M1 produces the two lower sidebands $f_1 - f_L$, $f_L - f_2$. These are separated by bandpass filters, and one of them is amplified to a level sufficient to serve as the LO for M2. M2 is an upconverter. Hence, its output phase is

$$\phi_i = (\phi_1 - \phi_L) + (\phi_L - \phi_2) = \phi_1 - \phi_2. \tag{6}$$

Since

$$\phi_1 = \omega_1 (t - r/c),$$

and

$$\phi_2 = \omega_2 (t - r/c),$$

Eq. (4) gives

$$\phi_i = (\omega_1 - \omega_2) (t - r/c),$$

in fulfillment of our requirement that the IF phase be an accurate representation of the pilot signal phase (or phases) uncontaminated by the phase of extraneous signals (the LO phase in this case).

Note that f_L in Figure 8b must not be exactly half way between f_1 and f_2, because then $f_1 - f_L$ would be equal to $f_L - f_2$ which would produce degeneracy in mixer M2. f_L need not be between f_1 and f_2, but if it isn't, mixer M2 must be a downconverter. The limiter in Figure 8b is required to avoid phase offset changes in the mixer M2 produced by changes in its input level.

C. Pointing Errors in ARA's

1) Doppler Errors: Doppler errors arise in two ways: first, from the radial velocity v_0 of the reference element with respect to the pilot source, and second, from the difference $v_k - v_0$ between the radial velocities of the kth and reference elements. In [1, appendix A] we derive an expression for $\delta\phi_{jk}$, the difference in phase between the contributions to the field at the pilot source, as a function v_0, v_j and v_k for $j, k = 1, \ldots, n$. Perfect retrodirection is, of course, equivalent to $\delta\phi_{jk} = 0$ for all pairs of elements j and k.

83

Considering first the error due only to the radial motion of the reference element, we get

$$\delta\phi_{jk} = \left(\frac{2\omega\nu_0}{c}\right)(\tau_k - \tau_j),$$ (5)

where

$$\tau_i = \left(\frac{1}{c}\right)r_i(t - \tau_i), \quad i = j, k$$

is the phase-delay time for the signal from the ith element arriving at the pilot source ($r = 0$) at time t. For a planar array

$$\tau_k - \tau_j = \left(\frac{1}{c}\right)a_{jk} \sin \theta,$$

where a_{jk} is the distance between the jth and kth elements, and θ is the scan angle, i.e. the angle of incidence of the pilot signal (Fig. 9). In [1, appendix A] we show that the transmitted beam points in the direction θ' given by

$$\sin \theta' = \left(1 + \frac{2\nu_0}{c}\right)\sin \theta$$ (6)

which gives

$$\Delta\theta = \theta' - \theta = \left(\frac{2\nu_0}{c}\right)\tan \theta.$$ (7)

Equation (7) is just the squint error due to the two-way Doppler shift

$$\Delta\omega = -\left(\frac{2\nu_0}{c}\right)\omega.$$

To get some idea of the magnitude of this error, apply (7) to the SPS ARA described in Section I. Its allowable pointing error is 17.6×10^{-6} rad. Therefore, assuming $|\theta| < 45°$ (much larger than the scan angles specified in ARA preliminary designs), (7) gives

$$\max \ |\nu_0| = 2640 \text{ m/s}.$$

The actual radial velocities of geosynchronous satellites are much smaller than this (less than 1.0 m/s in most cases), so we need not worry about "Doppler squint" for SPS.

The expression for the differential Doppler error is

$$\delta\phi_{oK} = \left(\frac{2\omega}{c}\right)\tau_{Ko}(\nu_0 - \nu_K),$$ (8)

where τ_{Ko} is the transmission line delay between the kth and reference elements. Since it depends on the value of each ν_K rather than just ν_0, the effects of differential Doppler are far more various than that of simple translational Doppler. In the absence of information on the various physical properties of the ARA structure and on its attitude control system, we have no way of knowing what steady-state or transient motions of the ARA are possible, and therefore, no way of applying (8). The best we can do is to calculate bounds on $|\nu_0 - \nu_K|$ based on a reasonable bound for τ_{Ko} and an arbitrary $|\delta\phi_{oK}|$ bound. A bound for $\tau_{Ko} = l_{Ko}/c_L$ is $\tau_{Ko} < 3D/2c$, which results if we assume that $l_{Ko} < D$, the dimension of the ARA, and $c_L > (2/3)c$. Let $\delta\phi$ be the

allowable phase error. Then from (8)

$$|\nu_0 - \nu_\kappa| \leq \frac{\lambda c(\delta\phi)}{6\pi D},$$

which says that the upper bound for the differential Doppler is proportional to the approximate beamwidth λ/D as well as to $\delta\phi$. Using the SPS antenna as an extreme example again, assume $D = 1000$ m, $\lambda = 0.125$ m, and $\delta\phi = 0.1\pi$. Then $|\nu_0 - \nu_\kappa| \leq 625$ m/s. Since such large relative velocities would be most unusual for any spacecraft, a differential Doppler will rarely, if ever, be significant.

2) <u>Aberration Error</u>: It can be shown [1, appendix B] that the transverse component ν_T of the ARA relative to the pilot source produces a pointing error

$$\Delta\psi = -\frac{2\nu_T}{c}. \tag{9}$$

We shall call this error an "aberration" because it is essentially the same phenomenon as an astronomical aberration: the small annual oscillation in the apparent position of stars due to the earth's orbital motion. Equation (9) is just twice the astronomical value, as one might expect from the fact that retrodirectivity is a two-way light path process, while the light from a star reaches the earth by a direct one-way path.

In Fig. 10 we assume that the spacecraft carrying the ARA moves with uniform velocity ν with respect to the pilot source. Equation (9) is obtained by applying the coordinate transformations of special relativity twice: first to obtain the angle of incidence of the pilot signal with respect to the ARA, and the second to obtain the angle of incidence of the retrodirected signal with respect to the pilot source.

The aberration error is negligible for geosynchronous satellites. For the 1.0-km diameter ARA of the SPS, the maximum allowable error, 17.6×10^{-6} rad, would be exceeded only by

$$\nu_T = 17.6 \times 10^{-6}(3 \times 10^8) = 2640 \text{ m/s},$$

whereas $\nu_T < 10$ m/s for the typical geosynchronous satellite.

3) <u>Effect of Transmission Line Mismatches</u>: Our previous analysis of central phasing (Section II-A) assumed that the phase shift produced by a transmission line of length l is simply $-\beta l$ for a signal of frequency $\omega = \nu_p \beta$, where the phase velocity ν_p is assumed to be independent of ω. But this result does not take into account the effect of multiple internal reflections in the line due to mismatches at its junctions with the diplexers at either end. When we do so (1, pp. 18-20), we find that the resulting error in the phase of the conjugate signal is approximately

$$\Delta\phi_b(l) = \arg(T_{1b}T_{2b}) - \frac{\omega_b}{\omega_a}\arg(T_{1a}T_{2a}) \tag{10}$$

where T_{1a}, T_{1b} are the voltage transmission coefficients at one end of the line at the pilot ω_a and conjugate ω_b frequencies, respectively, and T_{2a}, T_{2b} are the corresponding coefficients at the other end.

4) <u>Multipath Effects</u>: Multipath causes pointing errors in much the same way transmission line mismatches do. The received signal, either pilot or retrodirected, is the vector sum of a direct signal plus one or more signals each of which reach the receiving antenna after one or more reflections from the surroundings. The effect is to perturb the phase of the received signal. This would be harmless if $\omega_b = \omega_a$, for then reciprocity would assure exactly the same phase perturbation of the retrodirected signal received back at the pilot source no matter how complicated the multipath situation. But since $\omega_b \neq \omega_a$, reciprocity does not hold and phase errors result. Except in the very simplest cases, multipath effects are too difficult to calculate. Their presence can be inferred, however, by an irregular variation of the pointing error with a scan angle. We will see such evidence of multipath below in data obtained for a breadboard ARA.

5) Ionospheric Effects

Since they violate two necessary conditions for the operation of ARA's, ionospheric dispersion and time fluctuations are potential sources of pointing error. Ionospheric dispersion <u>per se</u> produces negligible pointing errors even at very high electron densities, but the <u>variation</u> of density across the region of the ionosphere traversed by the pilot signal may cause <u>differential</u> phase errors across the ARA aperture. These inhomogeneities of the ionosphere cause the scintillations occasionally observed in communication satellite signals. Their effect on ARA performance is now being investigated by Dr. A.K. Nandi of Rockwell and others. The possibility that absorption of SPS downlink power by the ionosphere may promote inhomogeneities is a further complication. Some ionospheric heating experiments have been made in this connection, but realistic simulation of this effect is impractical due to the huge volume and power of the SPS beam. The effect of a disturbed ionosphere on ARA performance is the chief unresolved problem in pointing the SPS beam. However, we can certainly say that no beam pointing system is immune to ionospheric effects, and no system so far proposed offers any better hope for dealing with it than does the ARA.

III. EXPERIMENTAL RESULTS

A. X-Band ARA

A two-element X-band ARA breadboard was built and tested by the author at the Jet Propulsion Laboratory. The purpose of the breadboard was to demonstrate exact phase conjugation and central phasing, both of which, as we saw above, would be necessary features of very large ultraprecise ARA's.

The PCC used in this breadboard is just that of Fig. 6 for n = 4, so that the frequency translation ratio is R = 2. Since this array has only two elements, both of which must transmit a conjugate signal, one of the elements must serve as reference element both for the other element and for itself.

The antenna range setup is shown in Fig. 11. The ARA is mounted on the antenna positioner on the right which rotates only in azimuth. The two ARA elements are identical rectangular horns mounted at the same height $23.2 \lambda_T = 82.4$ cm apart, where $\lambda_T = 3.55$ cm is the transmitted wavelength. The 3-dB beamwidth of the horns is about 30°. The rack on the left is the pilot source. A test receiver diplexed to the pilot horn provides the signal for the pattern recorder. The distance between the ARA and the pilot source is about 10 m. A considerable amount of absorbing material is required to minimize reflections in this very compact range.

The ARA pattern is shown as the dashed curve in Fig. 12; i.e., this curve is the output of the test receiver diplexed to the pilot horn as a function of ARA rotation in azimuth. An interferometer pattern (solid curve), produced by driving both elements from the same source at f_T = 8434.04 MHz, is superimposed on the ARA pattern by way of comparison. If the ARA were perfectly retrodirective, the dashed curve would be the envelope of the interferometer pattern over the entire scan, but, as we can see, this is true only within about ±5° of broadside. The main reason for the increasing departure from perfect retrodirectivity for scan angles greater than 5° is the increase in the multipath contribution to the signals received by both the ARA horns and the diplexed pilot horn at large scan angles. The effect of multipath is probably aggravated by amplitude-to-phase conversion in the ARA electronics. This conclusion is qualitatively supported by the fact that retrodirectivity dramatically improved when 1) the setup was reoriented to minimize reflections from nearby buildings, and 2) absorbing panels and material were placed in front of and on the reflecting surfaces as shown in Fig. 11.

The central phasing concept is incorporated into the ARA breadboard by connecting the second element to its PCC at the reference element by a coaxial line. A line stretcher included in this coaxial line enabled us to make an experimental check of that concept. The results of changing the line length are shown in Fig. 13. The ARA patterns for the indicated line-length changes were recorded in top-to-bottom time sequence starting with the zero line-length change (Δl = 0 in) pattern as a datum. The other two Δl = 0 patterns (between 2 in and 3 in and between 3 in and 4 in) were run as checks on thermal drift.

We see from Fig. 13 that Δl < 2 in does not appreciably affect the retrodirectivity of the ARA, while extending Δl to 3 in almost completely destroys it. The similarity of the three Δl = 0 patterns shows that thermal drift is not a factor in these measurements. The fact that Δl = 2 in = 1.43 wavelengths at f_T = 8.434 GHz shows that central phasing is highly effective in spite of the poorly matched rudimentary diplexers used in this breadboard.

B. 8 Element S-Band ARA

Figure 14 is a block diagram of the 8 element ARA now being built at JPL. Its transmitted frequency will be the same as that of the SPS, 2.45 GHz. It will employ the phase locked PCC of Figure 6 with n = 8 (R = 4/3), and the two-tone receiver of Figure 8b. A phase reference regenerator (PRR) similar to that of Figure 7 will be incorporated in the rudimentary, 2-node, central phasing tree. Preliminary bench tests have verified satisfactory performance of the PRR. Tests of this breadboard ARA are scheduled for this summer.

References

1. JPL Publication 78-20, "Large Active Retrodirective Arrays for Space Applications," Jet Propulsion Laboratory, Pasadena, CA.
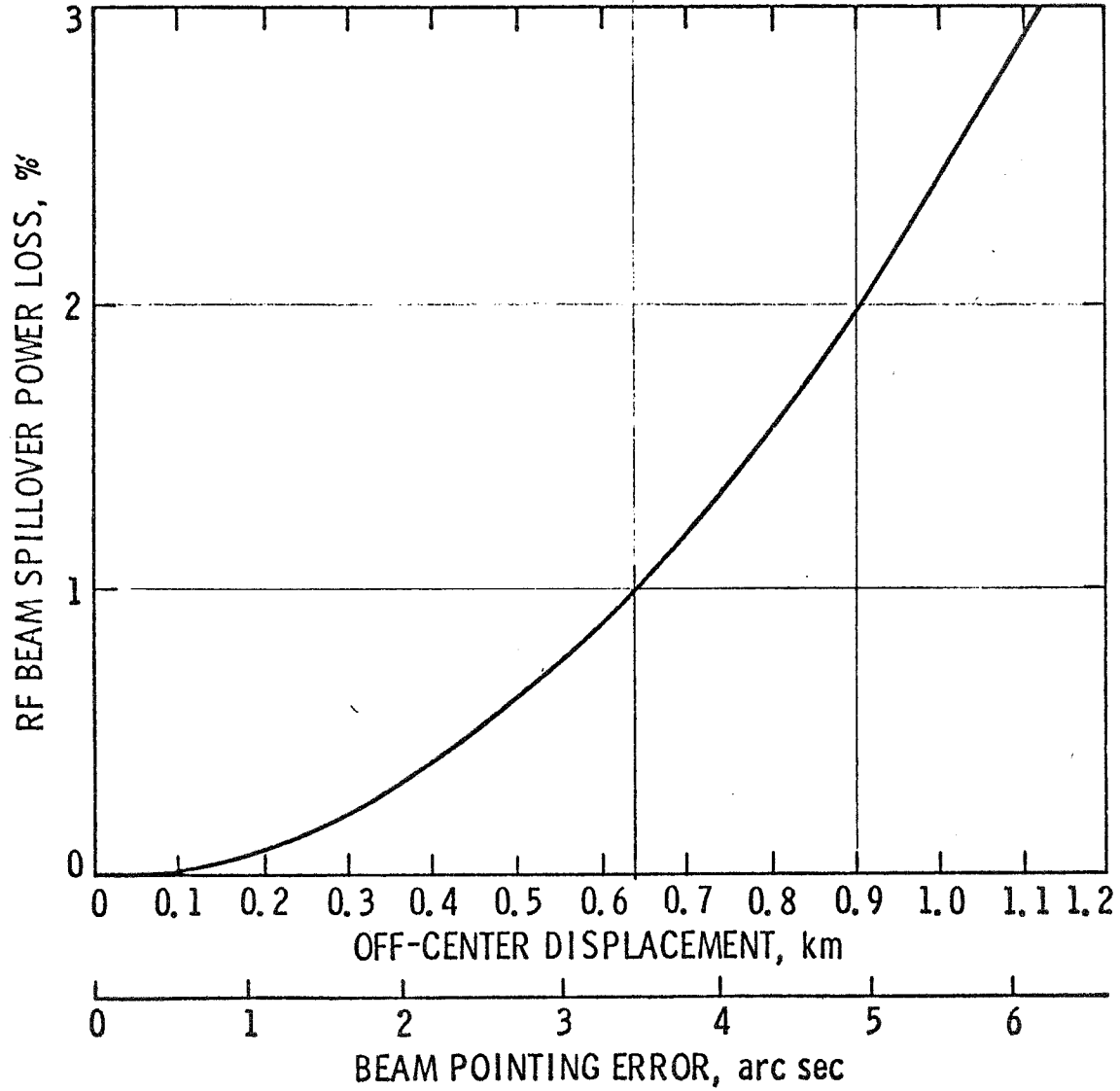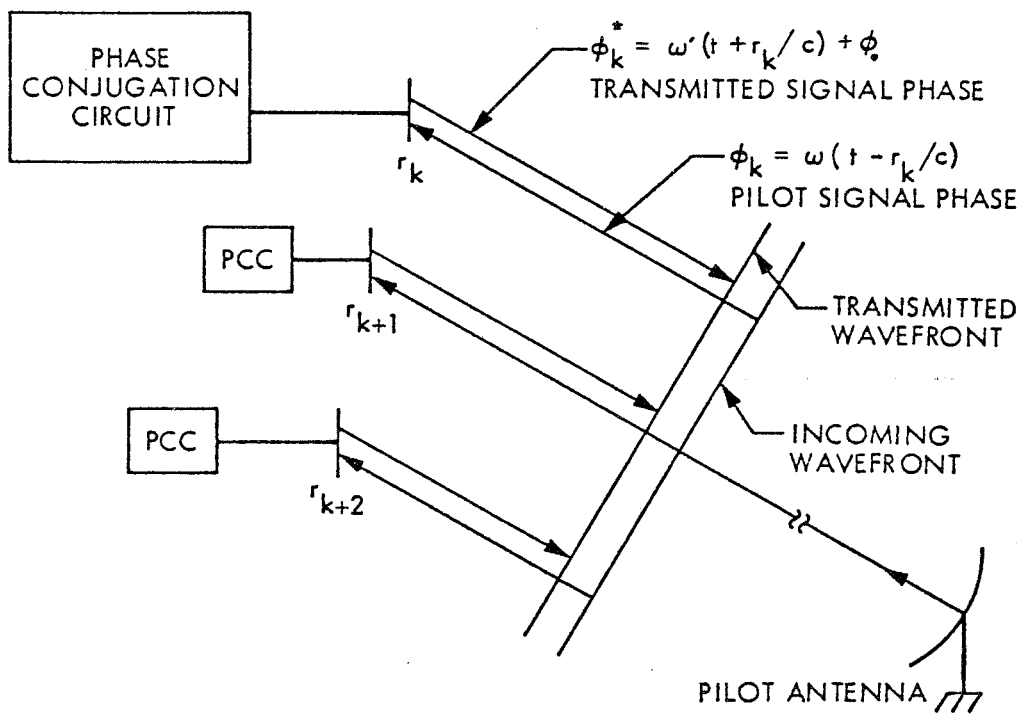
SPS BEAM POINTING LOSS

Figure 1.

PHASE
CONJUGATION
CIRCUIT

$\phi_k^* = \omega'(t + r_k/c) + \phi_{\bullet}$
TRANSMITTED SIGNAL PHASE

$\phi_k = \omega(t - r_k/c)$
PILOT SIGNAL PHASE

r_k

PCC

r_{k+1}

PCC

r_{k+2}

TRANSMITTED
WAVEFRONT

INCOMING
WAVEFRONT

PILOT ANTENNA

FIGURE 2   ACTIVE RETRODIRECTIVE ARRAY

89

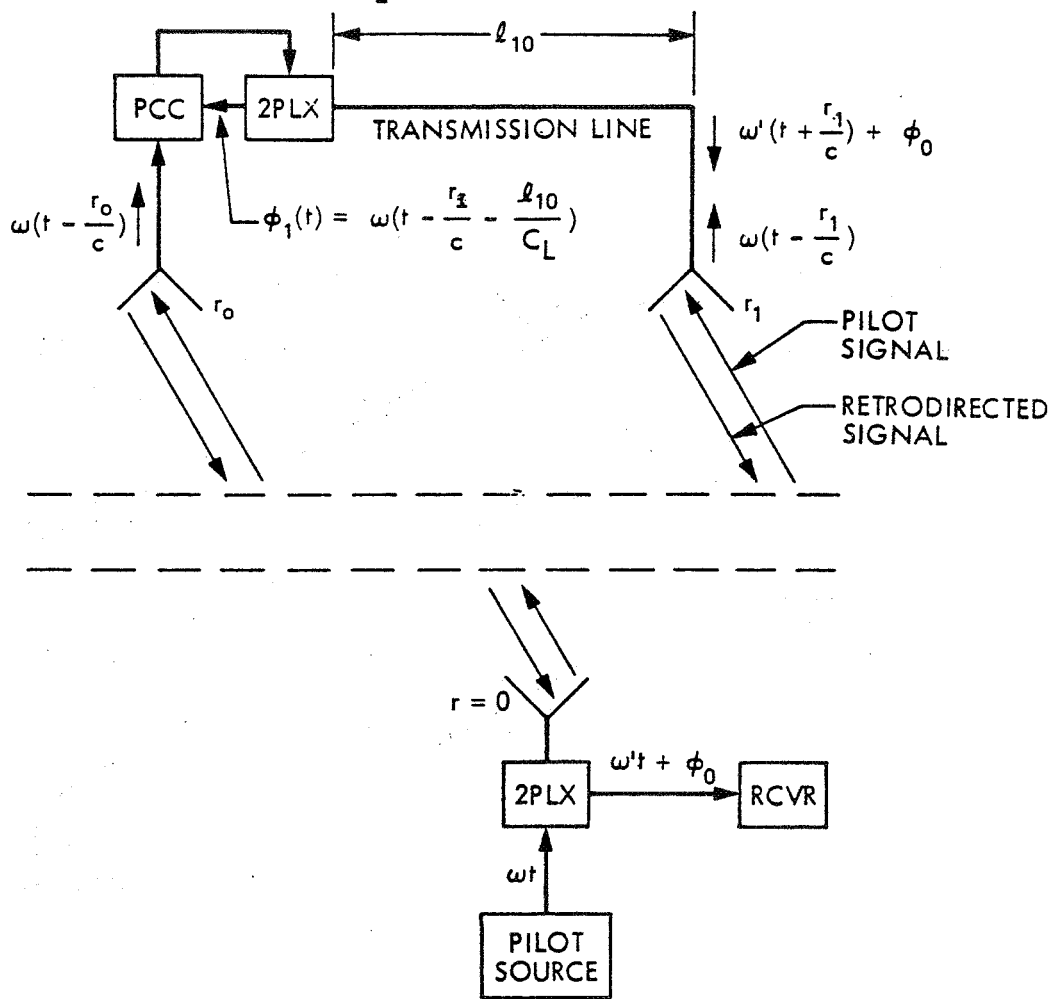$$[\phi_1(t)]^* = \omega'(t + \frac{r_1}{c} + \frac{\ell_{10}}{C_L}) + \phi_0$$

$$\leftarrow \ell_{10} \rightarrow$$

PCC $\leftarrow$ 2PLX TRANSMISSION LINE $\qquad \omega'(t + \frac{r_1}{c}) + \phi_0$

$$\omega(t - \frac{r_0}{c}) \uparrow \qquad \phi_1(t) = \omega(t - \frac{r_1}{c} - \frac{\ell_{10}}{C_L}) \qquad\qquad \omega(t - \frac{r_1}{c})$$

r_0

r_1

PILOT
SIGNAL

RETRODIRECTED
SIGNAL

$r = 0$

2PLX $\qquad \omega't + \phi_0 \qquad$ RCVR

ωt

PILOT
SOURCE

FIGURE 3 CENTRAL PHASING

90
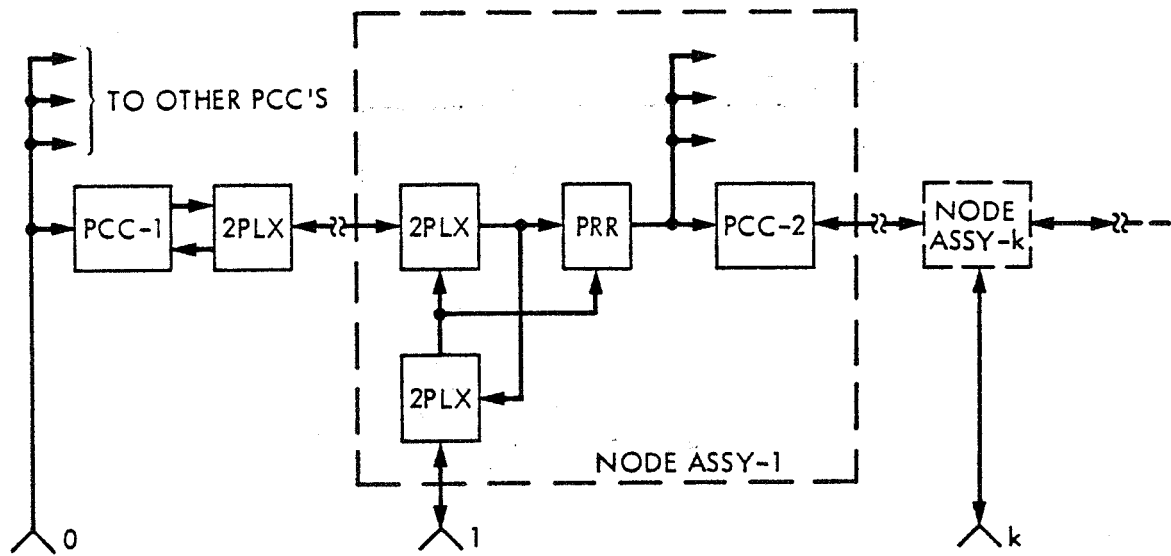
FIGURE 4. TREE STRUCTURE FOR CENTRALLY PHASED ARA

$\phi_{REF} = 2\omega t + \phi_0$

$\phi_i^* = \omega(t + \frac{r}{c}) + \phi_0$

$\phi_i = \omega(t - \frac{r}{c})$

REF
2ω
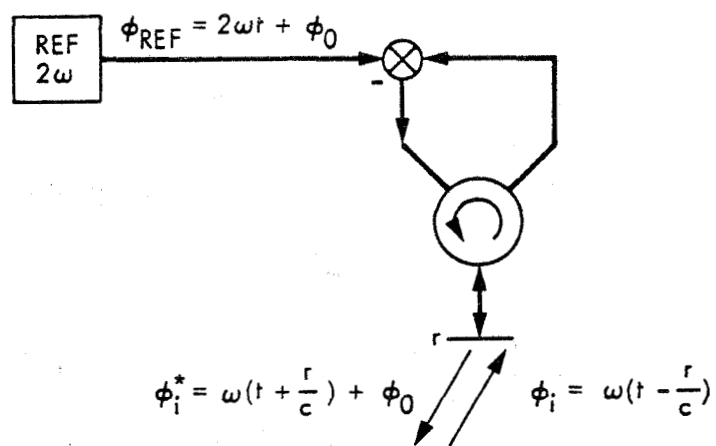
FIGURE 5. SIMPLE PHASE CONJUGATING CIRCUIT
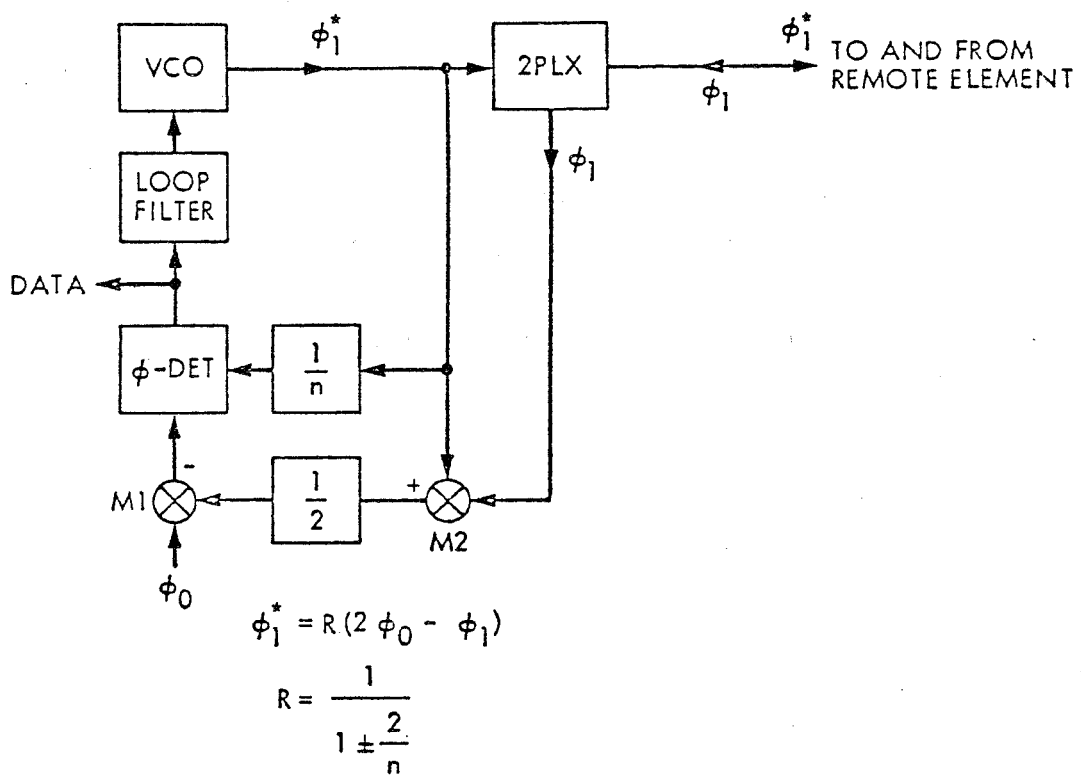
FIGURE 6. EXACT PCC: PHASE LOCKED LOOP TYPE
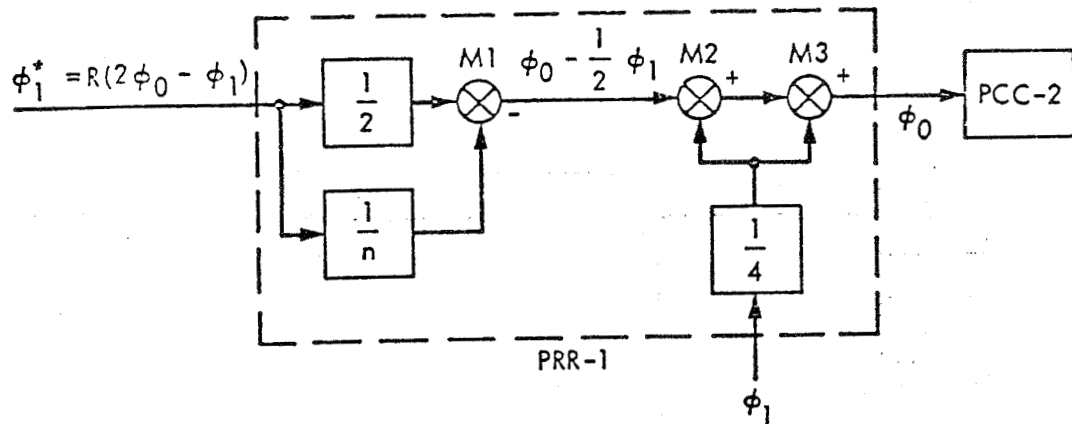
FIGURE 7. PHASE REFERENCE REGENERATOR (PRR) FOR PCC OF FIGURE 6

PILOT: $f_1 \angle \phi_1$ → ⊗ → [IF] f_i → [ϕ-DET] → [LOOP FILTER] → [VCO] → f_i → TO PCC

nf_i ← [×n] ←

$f_i \angle \phi_i$

$$\phi_i = \frac{\phi_1}{n+1} = \frac{-\omega_1 \, r}{(n+1)c}$$
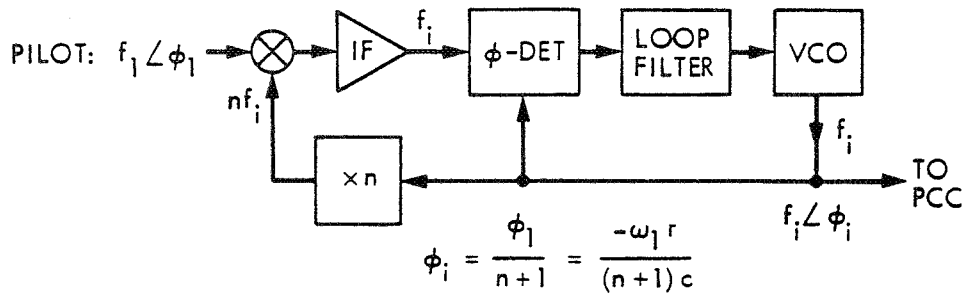
PHASE LOCKED LOOP RECEIVER

(a)

RF MIXER

$f_1, \, f_2$ → ⊗ → [BPF f_1'] → ⊗ $+$ → [BPF f_i] → TO PCC $f_i \angle \phi_i$

f_{LO}

HYBRID

[BPF f_2'] → ▷ LIMITER AMP.

RF SPECTRUM

f_2 f_{LO} f_c f_1

IF SPECTRUM
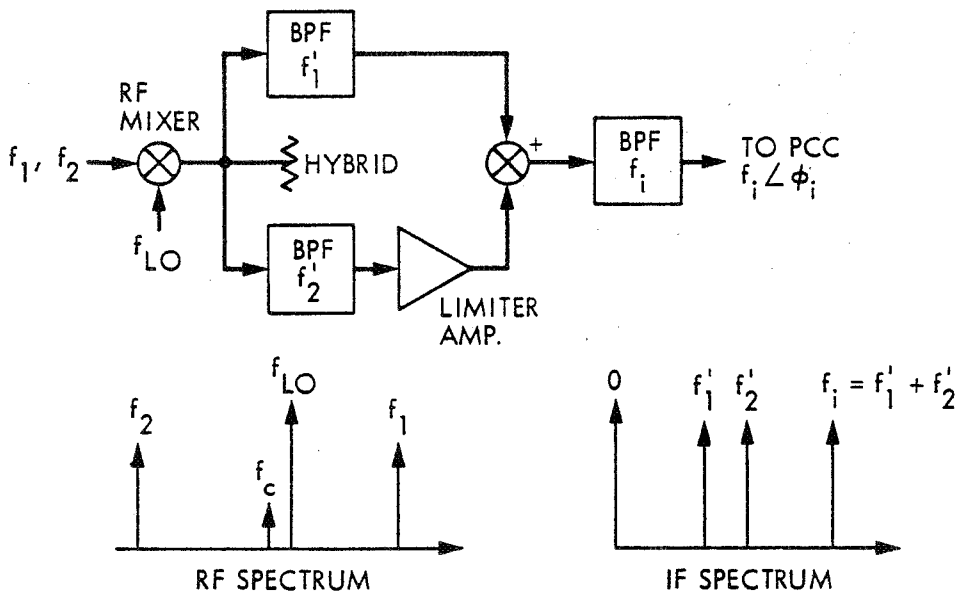
0   f_1' f_2' $f_i = f_1' + f_2'$

$$f_1' = f_1 - f_{LO}$$

$$f_2' = f_{LO} - f_2$$

$$f_i = f_1' + f_2' = f_1 - f_2$$

$$\phi_i = \phi_1 - \phi_2 = (\omega_2 - \omega_1)\frac{r}{c}$$

TWO TONE RECEIVER

(b)

FIGURE 8. ARA RECEIVERS

95
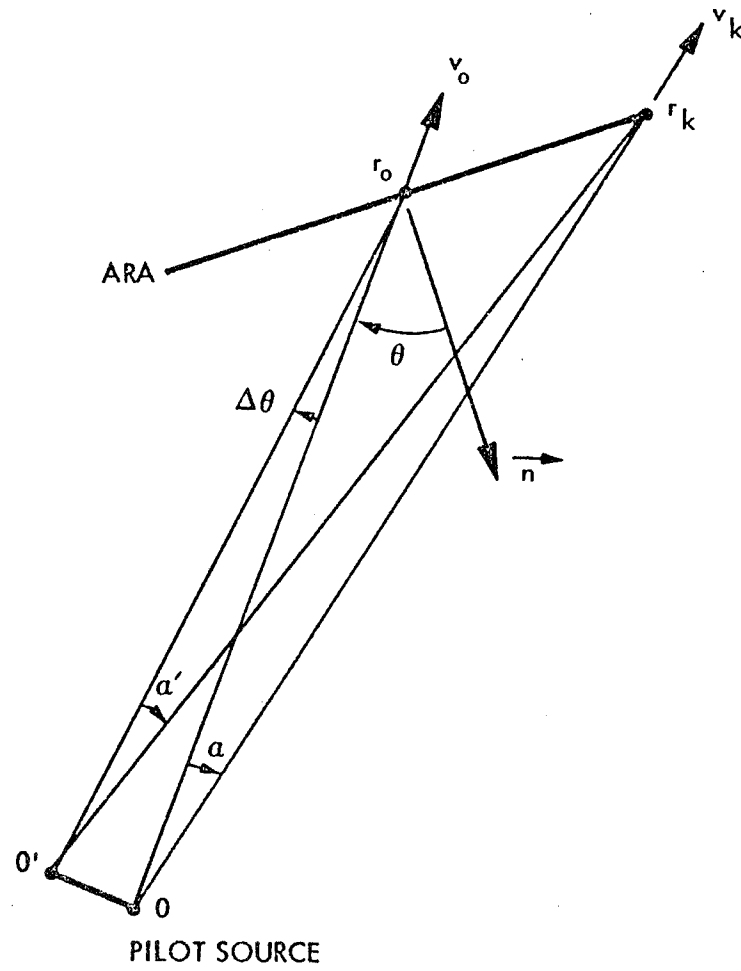
FIGURE 9. DOPPLER POINTING ERROR
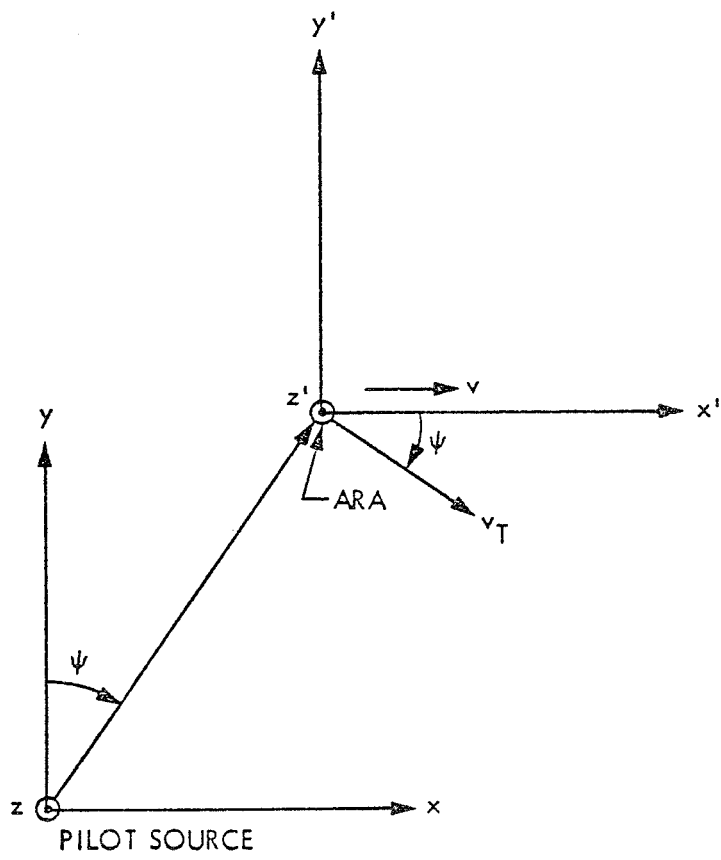
FIGURE *10*. ABERRATION POINTING ERROR
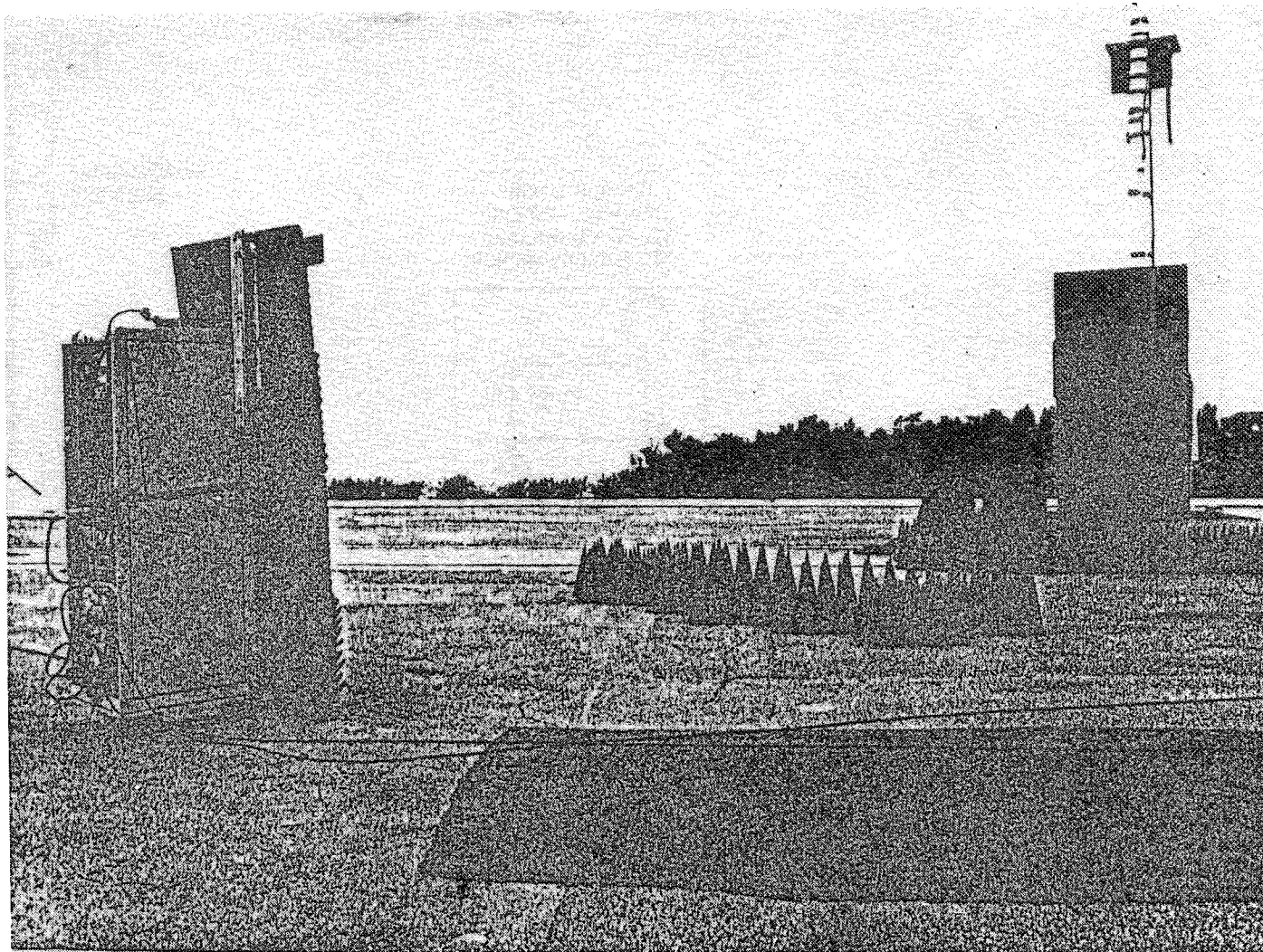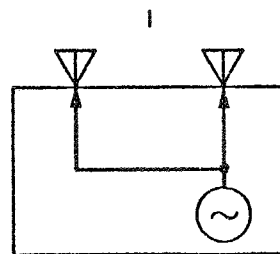
Figure 11. Antenna Range Set-up

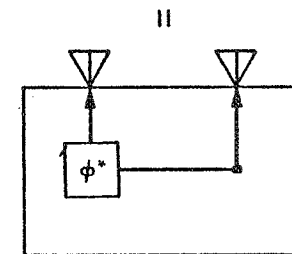LEGEND:

DIPLEXED PILOT HORN

ARA ON POSITIONER
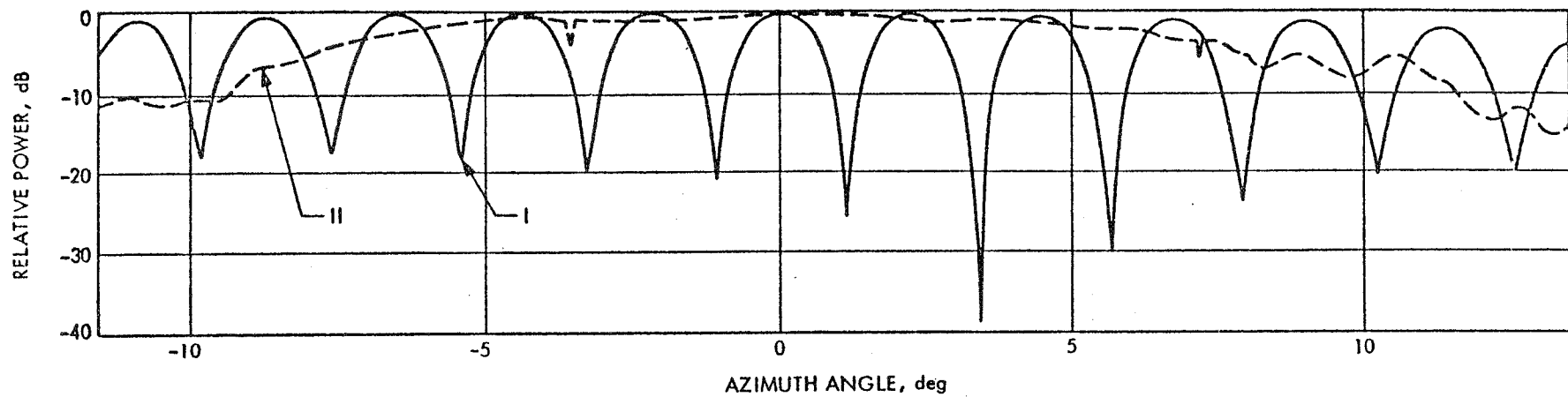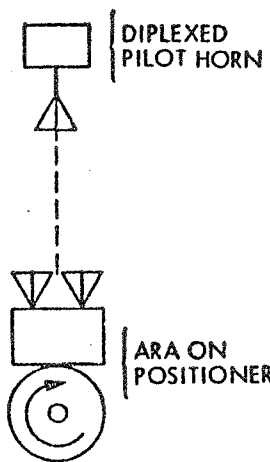
PATTERN RANGE CONFIGURATION

I

REF.-REMOTE INTER-FEROMETER (SAME SOURCE DRIVING BOTH HORNS)

II

ACTIVE, RETRO-DIRECTIVE ARRAY (ADDED PHASE CONJUGATOR CIRCUITRY)
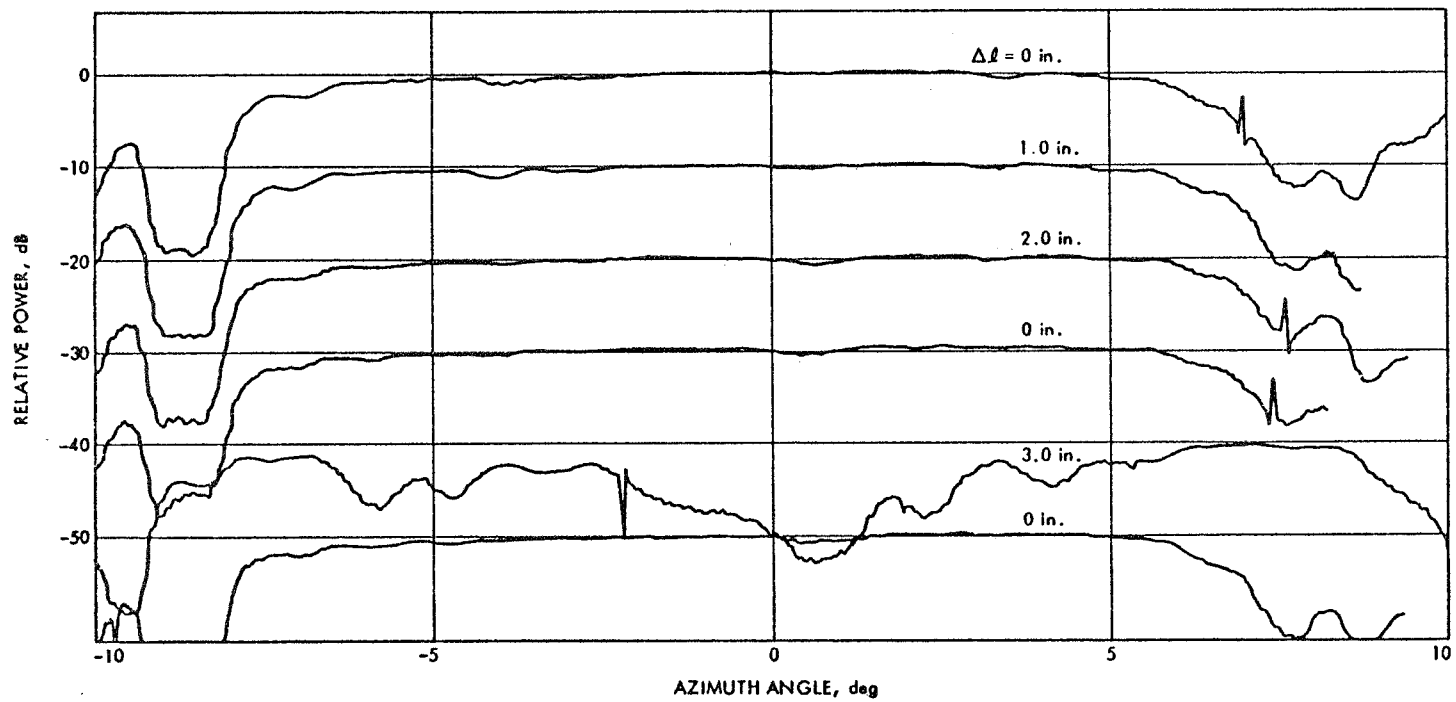
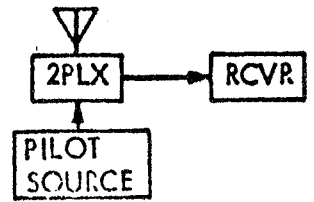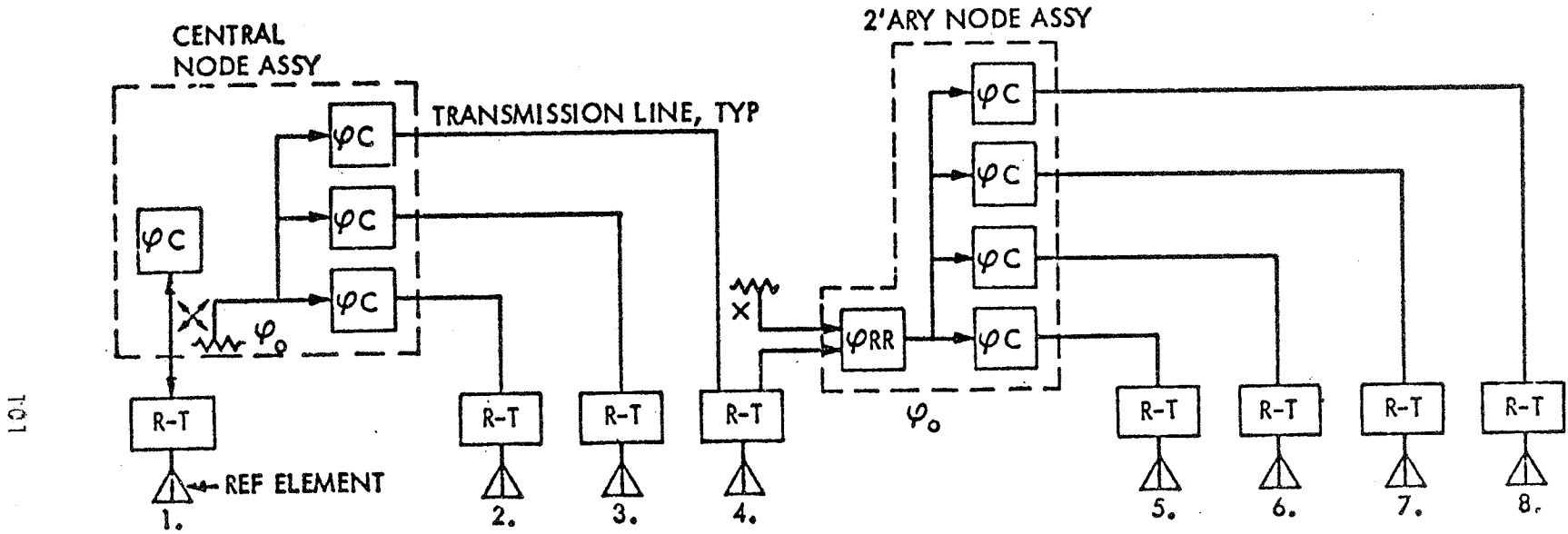FIGURE 12. RETRODIRECTIVE ARRAY PATTERN

FIGURE /3. ARA BREADBOARD: EFFECT OF LINE LENGTH CHANGES

BEAMED RF POWER TECHNOLOGY
8-ELEMENT EXPERIMENTAL ACTIVE
RETRODIRECTIVE ARRAY (ARA) BLOCK DIAGRAM

Figure 14.

LEGEND:
R-T = RCVR-XMTR-DIPLEXER ASSY
φC = PHASE CONJUGATOR
φRR = PHASE REFERENCE REGENERATOR
φ_0 = REFERENCE PHASE
2PLX = DIPLEXER